accompanied by a second branch in the second layer (arrow b), the two branches being oriented in opposite directions. The number of layers in the upper and lower regions is 10 and 9, respectively (white arrows). The extra top layer terminates near to the branching point (arrow c). If one ignores this extra layer, the two branch structures do not generate any additional layers between adjacent layers (i.e. similar to a dislocation). Meanwhile, the 6.2 Å *d*-spacing is well-maintained across the branching layers. In the triple-layered MS_2 structure only M–S bonds exist, not M–M or S–S bonds. Therefore, it is possible that the upper S–M and lower M–S layers split, accompanied by two additional S layers formed at the splitting point (Fig. 4b).

Table 1 lists the Raman bands of $W_xMo_yC_zS_2$ nanotubes and their assignments. WS_2 bands are also listed for comparison, the Raman spectra being recorded using 514.5 and 632.8 nm excitation. With 514.5 nm excitation, the sample burned readily, so a low laser power had to be used and only the three strongest Raman bands were observed. With 632.8 nm excitation, the spectrum of $W_xMo_yC_zS_2$ (Fig. 5) is similar to that of WS_2 [6], the main difference being the increased intensity of the 176, 198 and 211 cm^{-1} bands relative to that of the 297 cm^{-1} band. This is consistent with the 176 cm^{-1} band being assigned to a disorder-induced mode. The presence of C–C bonds leads to disruption of the MS_2 lattice, so that the 176 cm^{-1} band intensity increases. The increase in the relative intensity of the previously unassigned bands at 198 and 211 cm^{-1} implies that they are also due to disorder-induced modes: a similar conclusion was reached for a band seen at 192 cm^{-1} in the Raman spectrum of $W_{0.9}Nb_{0.1}S_2$ [7]. Possible combinations of the 198 and 211 cm^{-1} bands with the intense a_g^1 band are also seen in this spectrum.

Acknowledgements

We thank the Leverhulme Trust, the Royal Society and the ULIRS for financial support.

References

[1] Hsu WK, Zhu YQ, Boothroyd CB, Kinloch I, Trasobares S, Terrones H et al. Chem Mater 2000;12:3541.
[2] Hsu WK, Chang BH, Zhu YQ, Wei QH, Terrones H, Terrones M et al. J Am Chem Soc 2000;122:10155.
[3] Hoistad LM, Meerschaut A, Bonneau P, Rouxel J. J Solid State Chem 1995;114:435.
[4] Iijima S. Nature 1991;354:56.
[5] Hsu WK, Zhu YQ, Trasobares S, Terrones H, Terrones M, Grobert N et al. Appl Phys A 1999;68:493.
[6] Frey GL, Tenne R, Matthews NJ, Dresselhaus MS, Dresselhaus G. J Mater Res 1998;13:2412.
[7] Zhu YQ, Hsu WK, Terrones M, Firth S, Grobert N, Clark RJH et al. Chem Commun 2001:121–2.

Porous texture of activated carbons prepared by phosphoric acid activation of apple pulp

F. Suárez-García, A. Martínez-Alonso, J.M.D. Tascón*

Instituto Nacional del Carbón, CSIC, Apartado 73, 33080 Oviedo, Spain

Received 13 February 2001; accepted 23 February 2001

Keywords: A. Activated carbon; B. Activation; C. Adsorption; D. Porosity; Surface areas

Apples constitute one of the most abundant fruits, with a world production of 53.2 million metric tons (Mt) in 1997 and a forecast of 68.3 Mt for 2005 [1]. Although apples are principally consumed directly as a fruit, about 12% of the production is destined to the manufacture of apple juice and cider [2]. In turn, the solid residue from pressing apples (apple pulp) represents more than 12 wt.% of the fruit [3]. Therefore, taking an intermediate value of 60 Mt for the yearly world production, about 0.84 Mt of apple pulp are generated yearly worldwide. Although it is not as polluting as other vegetable by-products from the food industry, apple pulp is a useless material that is often spilled in a non-controlled way. This work concerns the porous texture characteristics of activated carbons (ACs) prepared by chemical activation of apple pulp. To the authors' knowledge, this product has never been used previously as a feedstock to prepare activated carbons by chemical activation [4].

*Corresponding author. Tel.: +34-98-528-0800; fax: +34-98-529-7662.

E-mail address: tascon@incar.csic.es (J.M.D. Tascón).

0008-6223/01/$ – see front matter © 2001 Elsevier Science Ltd. All rights reserved.
PII: S0008-6223(01)00053-7

The char yield of apple pulp (~25 wt.% at 1073 K) [5] is similar to those found for other biomass products; for instance, Mourão et al. [6] reported a char yield of 21–25 wt.% for cork oak at 1073 K. Raveendran et al. [7] indicated that the char yield of a wide variety of lignocellulosic materials at 1273 K varies between 18 and 35 wt.%. In previous works [5,8,9] we used thermogravimetry to explore the possibility of increasing the char yield of apple pulp by modifying the pyrolysis conditions, and also to assess the effect of various additives known to affect biomass pyrolysis. We observed that only phosphoric acid produced an increase in the char yield. Therefore, we have selected this additive for further assessment as an activating agent. Indeed, H_3PO_4 is widely used in the preparation of carbon adsorbents from lignocellulosic products [10–13], and offers some advantages such as nonpolluting character (compared to $ZnCl_2$, for instance) and ease of elimination by leaching with water, thereby recovering H_3PO_4 that can be recycled for further use.

The apple pulp used in this work was a solid residue from pressing crushed apples for cider production. The apple mixture was representative for those typically used in the production of Asturian cider. As-received apple pulp was spread on metal trays and allowed to dry in air for 15 days at room temperature followed by 6 days at 308 K under forced air circulation, the weight loss it underwent in the entire process being 75.8%. To homogenize the dried material it was ground (using a knife mill) to pass a sieve of 1 mm and thoroughly mixed. Proximate analysis of apple pulp (wt.%, dry basis: db) gave 5.7% moisture, 79.0% volatile matter, 2.6% ash and 3.3% inorganic (mineral) matter. Elemental analysis (wt.%, db) gave 49.56% C, 8.43% H, 0.97% N, 0.05% S and 38.22% O. Biopolymer analysis (wt.%, db) gave 43.99% hollocellulose, 17.32% lignin, 6.66% solubles in organic solvents and 31.33% solubles in water. The standard methods followed in these analyses are specified elsewhere [5]. The low inorganic matter and sulfur contents are particularly favorable factors for the use of apple pulp as a feedstock for AC production.

Apple pulp was impregnated with aqueous solutions of H_3PO_4 following a variant of the incipient wetness method, as described elsewhere [5], consisting of adding dropwise (while stirring the solid, to facilitate homogeneous absorption of liquid) the amount of aqueous solution (3.5 cm^3/g apple pulp) necessary to produce swelling until incipient wetness. After impregnation, the samples were dried for 4 h at 383 K in air. Different concentrations of H_3PO_4 in the aqueous solutions were used to vary the content of impregnating agent, which is expressed as impregnation ratio (X_p, wt.%), defined as (g H_3PO_4/g apple pulp)$\times$100. Impregnation ratios of 21, 30, 43, 50, 64, 75, 85, 100, 125 and 150 wt.% were used. Activations were carried out in a vertical tubular reactor made from quartz, using in all cases 15 g of impregnated apple pulp. All treatments were done at a constant heating rate of 10 K min^{-1} and with an upwards argon (99.999% pure) flow of 50 STP cm^3 min^{-1}, which was kept during both heating and cooling. On the basis of preliminary experiments (not reported here), an activation temperature of 723 K and a soaking time of 1 h were selected. After cooling the solid pyrolysis residue to room temperature it was washed with milli-Q distilled water until lowering the conductivity of the washing liquids to <5 μS cm^{-1} (measured with a

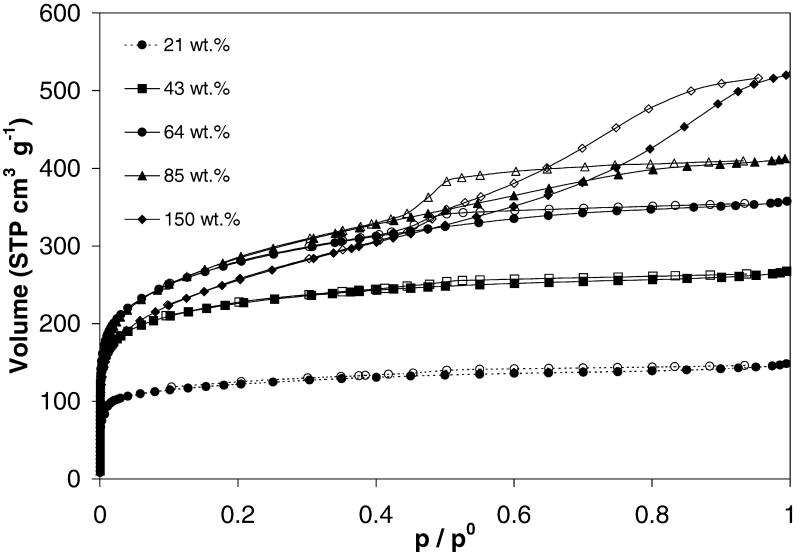

Fig. 1. Adsorption–desorption isotherms of N_2 at 77 K on ACs with different impregnation ratios. Full symbols, adsorption; open symbols, desorption.

pH/conductivity meter Mettler Toledo, model MPC227). The resulting ACs were dried for 12 h at 383 K in a vacuum furnace.

The porous texture of ACs was characterized by physical adsorption of nitrogen and carbon dioxide, using an automatic volumetric apparatus (ASAP 2010, Micromeritics) to measure N_2 isotherms at 77 K (relative pressure range of 10^{-6} to 0.99) and a semiautomatic volumetric adsorption apparatus (NOVA-1200, Quantachrome) to measure CO_2 isotherms at 273 K. In either case the samples were degassed overnight at 523 K before every adsorption measurement. Gases used had minimum purities of 99.999% (N_2) and 99.98% (CO_2). N_2 adsorption data were analyzed by means of the BET and Dubinin–Radushkevich (DR) equations and the α_S method (using Spheron 6 carbon black as reference material). The CO_2 adsorption data were analyzed using the Dubinin–Radushkevich–Kaganer (DRK) equation.

Fig. 1 shows N_2 adsorption–desorption isotherms at 77 K on a selection of ACs prepared from apple pulp impregnated with different amounts of H_3PO_4 and activated at 723 K with 1 h soaking time. For low impregnation ratios ($X_p < 43$ wt.%) the isotherms are type I, with practically no hysteresis, the materials being essentially microporous. For intermediate impregnation ratios (64–100 wt.%) the isotherms are still type I but the knee opens indicating widening of pores; a plateau is not clearly reached, indicating the presence of a wide range of pore sizes. These isotherms exhibit type H_4 hysteresis loops, typical for slit-shaped pores. Finally, the samples with highest impregnation ratios (125–150 wt.%) yielded isotherms intermediate between types I and II, with a hysteresis loop intermediate between types H_3 and H_4, indicating the presence of slit-shaped pores and a wide distribution of pore sizes [14]. Similar evolutions from type I to type II isotherms with increasing amount of H_3PO_4 have been reported by Molina-Sabio et al. [10] and Philip [15].

Fig. 2 shows α_S curves drawn from isotherms from Fig. 1 corresponding to samples with impregnation ratios of 21, 64 and 150 wt.%. Following the classification proposed by Sellés-Pérez and Martín-Martínez [16], the sample with $X_p = 21$ wt.% exhibits an α_S curve intermediate between types α-1a and α-2, indicating the presence of a rather narrow microporosity. The sample impregnated at 64 wt.% gives an α-2 type curve, usual for materials with a wide pore size distribution. Finally, the sample impregnated at $X_p = 150$ wt.% yields an α_S curve intermediate between the α-1b and α-1c types, indicative of a well-developed mesoporosity. Consequently, the α_S curves confirm that, as the amount of phosphoric acid used in the impregnation increases, a progressive widening of the micropores takes place, leading to wider pore size distributions.

Table 1 reports textural parameters deduced from N_2 and CO_2 adsorption. The BET (S_{BET}) and micropore [$S_{\mu p}$ (DR, N_2)] surface areas increase with increasing impregnation ratio until 64–85 wt.% and decrease afterwards. The external surface area, S_{ext} (α_S, N_2), increases with increasing X_p, slightly at low impregnation ratios and more steeply above 100 wt.% as could be expected from the shape of the isotherms. Concerning pore volume parameters, the total pore volume, V_p (0.975, N_2), goes through a relative maximum at 85 wt.%, then decreases until 100 wt.% and increases again (sharply) for the two samples impregnated with the largest amounts of phosphoric acid. The ultramicropore volume, $V_{u\mu p}$ (α_S, N_2) and the micro-

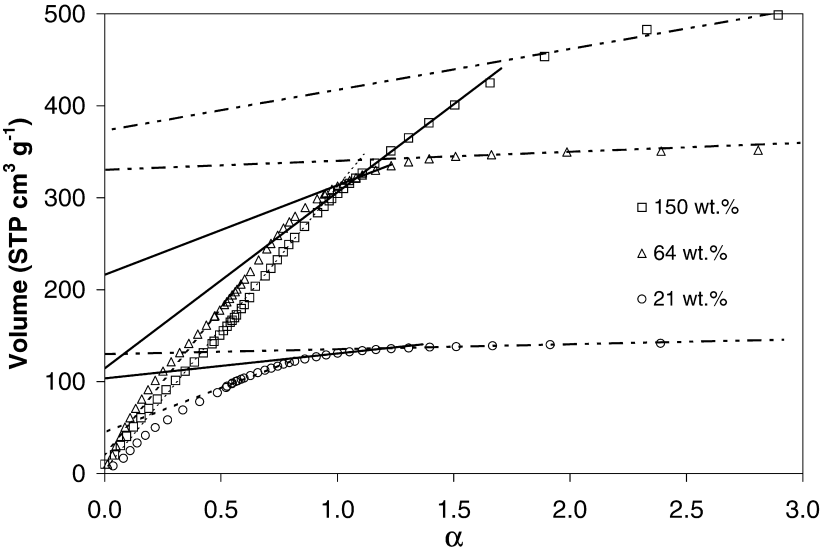

Fig. 2. α_S-plots drawn from N_2 adsorption isotherms on ACs with impregnation ratios of 21, 64 and 150 wt.%.

Table 1
Textural parameters deduced from N_2 adsorption at 77 K and CO_2 adsorption at 273 K on ACs with different impregnation ratios. Surface areas in $m^2\ g^{-1}$; pore volumes in $cm^3\ g^{-1}$

X_p	N_2							CO_2	
(wt.%)	S_{BET}	V_p	α_S-method			DR-method		DRK-method	
			S_{ext}	$V_{\mu pt}$	$V_{u\mu p}$	$S_{\mu p}$	$V_{\mu p}$	$S_{\mu p}$	$V_{\mu p}$
0	3	0.003	–	–	–	–	–	280	0.10
21	454	0.22	16	0.17	0.07	531	0.19	423	0.15
43	837	0.41	19	0.30	0.08	886	0.31	568	0.21
64	1010	0.55	28	0.31	0.03	1034	0.37	535	0.19
85	1022	0.63	27	0.29	0.01	1030	0.37	500	0.18
100	1011	0.60	37	0.27	0.00	1013	0.36	437	0.16
150	914	0.80	128	0.18	0.00	911	0.32	441	0.16

pore volume calculated from CO_2 adsorption, $V_{\mu p}$ (DRK, CO_2), reach maxima at $X_p = 43\%$. $V_{u\mu p}$ (α_S, N_2) is smaller than $V_{\mu p}$ (DRK, CO_2) for all samples, indicating the presence of very small pores to which N_2 has no access due to activated diffusion restrictions. The two micropore volumes calculated from N_2 adsorption, $V_{\mu pt}$ (α_S, N_2) and $V_{\mu p}$ (DR, N_2), evolve in parallel, attaining maxima at 64 wt.%. In the light of these results one can conclude that, at low impregnation ratios (below 43 wt.%), phosphoric acid promotes the development of porosity, principally micropores. At intermediate impregnation ratios, pores with a wide range of sizes, between ultramicropores and mesopores, are developed, with a tendency towards wider pores as the impregnation ratio increases. At impregnation ratios above 100 wt.% wide micropores and mesopores are formed. According to Jagtoyen and Derbyshire [12,13], the porosity is generated with phosphoric acid remaining intercalated in the internal structure of lignocellulosic materials, hindering their shrinkage. As the amount of H_3PO_4 used in the impregnation increases, the volume filled by it and the various polyphosphate structures will obviously increase, resulting in larger pore volume and pore size.

In summary, chemical activation of apple pulp with H_3PO_4 produces materials with a well-developed pore structure. Also, a reasonable yield (30–40 wt.% relative to dried apple pulp, or 7–10 wt.% relative to as-received, moist apple pulp) is achieved, suggesting the practical feasibility of the process. The amount of phosphoric acid used in the impregnation strongly influences the porous texture of the resulting ACs. At low impregnation ratios, phosphoric acid promotes the development of micropores. At intermediate and high impregnation ratios a progressive widening of the micropores takes place, with a tendency towards wider pores as the impregnation ratio increases. Therefore, ACs with wide micropores are obtained at an intermediate impregnation ratio, and ACs with a well-developed mesoporosity are obtained at high impregnation ratios (125–150 wt.%).

Acknowledgements

Financial support from II PRI Asturias (project PB-MAT98-01) and CICYT (project OLI96-2144) is gratefully acknowledged.

References

[1] O'Rourke AD. World apple marketing dynamics. http://impact.wsu.edu/impactreports.htm
[2] Alvarez Blanco S. Apple juice concentration by reverse osmosis: modelling and economic evaluation of the process, Oviedo, Spain: Oviedo University, 1998, Doctoral thesis.
[3] Marañón E. Heavy metals removal from industrial effluents using chemically modified apple residues and ion exchange resins, Oviedo, Spain: Oviedo University, 1990, Doctoral thesis.
[4] Suárez-García F, Martínez-Alonso A, Tascón JMD. Procedure for producing activated carbons from apple pulp. Spanish patent (application number: P00002214), 2000.
[5] Suárez-García F, Martínez-Alonso A, Tascón JMD. Pyrolysis of apple pulp: effect of operation conditions and chemical additives. J Anal Appl Pyrol 2001, in press.
[6] Mourão PAM, Carrott PJM, Ribeiro Carrott MML. Preparation of activated carbons from cork oak. In: Abstracts and programme, Eurocarbon 2000, vol. II, Berlin: DGK, 2000, pp. 639–40.
[7] Raveendran K, Ganesh A, Khilar KC. Pyrolysis characteristics of biomass and biomass components. Fuel 1996;75(8):987–98.
[8] Suárez-García F, Martínez-Alonso A, Tascón JMD. Apple pulp pyrolysis for the preparation of activated carbons. In: Communications, 5th Spanish Carbon Group Meeting, Oviedo, Spain: GEC, 1999, pp. 285–8.
[9] Suárez-García F, Martínez-Alonso A, Tascón JMD. Effect of operation conditions and chemical additives on apple pulp pyrolysis. In: Abstracts and programme, Eurocarbon 2000, vol. II, Berlin: DGK, 2000, pp. 537–8.
[10] Molina-Sabio M, Rodríguez-Reinoso F, Caturla F, Sellés MJ. Porosity in granular carbons activated with phosphoric acid. Carbon 1995;33(8):1105–13.

[11] Laine J, Calafat A, Labady M. Preparation and characterization of activated carbons from coconut shell impregnated with phosphoric acid. Carbon 1989;27(2):191–5.
[12] Jagtoyen M, Derbyshire F. Some considerations of the origins of porosity in carbons from chemically activated wood. Carbon 1993;31(7):1185–92.
[13] Jagtoyen M, Derbyshire F. Activated carbons from yellow poplar and white oak by H_3PO_4 activation. Carbon 1998;36(7–8):1085–97.
[14] Rouquerol F, Rouquerol J, Sing KSW. Adsorption by powders and porous solids. Principles, methods and applications, San Diego, CA: Academic Press, 1999.
[15] Philip CA. Adsorption characteristics of microporous carbons from apricot stones activated by phosphoric acid. J Chem Tech Biotechnol 1996;67(3):248–54.
[16] Sellés-Pérez MJ, Martín-Martínez JM. Classification of α_S plots obtained from N_2/77 K adsorption isotherms of activated carbons. Fuel 1991;70(7):877–81.

Micropore sizes in activated carbons determined from the Dubinin–Radushkevich equation

F. Stoeckli[a,*], M.V. López-Ramón[b], D. Hugi-Cleary[a], A. Guillot[c]

[a]*Institut de Chimie de l'Université, Av. de Bellevaux 51, CH-2000 Neuchâtel, Switzerland*
[b]*Departamento de Química Inorgánica, Universidad de Jaen, E-23071 Jaen, Spain*
[c]*CNRS-IMP Université de Perpignan, 52 Avenue de Villeneuve, F-66806 Perpignan, France*

Received 14 February 2001; accepted 23 February 2001

Keywords: A. Activated carbon; C. Adsorption; Modeling; D. Adsorption properties; Microporosity

Microporous carbons are characterized by relatively heterogeneous pore size distributions (PSD), but their structure may be regarded as a collection of locally slit-shaped micropores [1–3]. Different techniques have been used to derive PSDs, in particular the use of molecular probes adsorbed from the vapour and the liquid phases [4] and, more recently, the analysis of adsorption data with the help of model isotherms resulting from computer simulations [5,6]. These studies provide information on the average micropore width L_o. Further evidence can be obtained from the adsorption of caffeine [4] and of phenol [7] from aqueous solutions and the corresponding enthalpies of immersion $\Delta_i H$. These molecules are adsorbed as type I isotherms, with limiting amounts N_{am}. The molar energies of transfer from the liquid to the solid, $\Delta_i H/N_{am}$, respectively -64 to -66 kJ mol^{-1} (caffeine) and -30 to -32 kJ mol^{-1} (phenol), are identical for non-porous and porous carbons. This suggests that the same mechanism takes place, i.e. the coating of the micropore wall area S_{mi} and/or of the non-microporous area S_e. The specific enthalpies of immersion h_i(caffeine) $= -0.113 \pm 0.010$ J m^{-2} and h_i(phenol) $= -0.109 \pm 0.008$ J m^{-2} obtained with carbon blacks, lead to the total surface area $S_{tot} = S_{mi} + S_e$. The average width L_o of slit-shaped micropores, is given by:

$$L_o\,(\text{nm}) = 2000\, W_o\,(\text{cm}^3\,\text{g}^{-1})/S_{mi}\,(\text{m}^2\,\text{g}^{-1}) \quad (1)$$

W_o being the volume filled. It has been shown that a correlation exists between L_o and the so-called characteristic energy E_o of the Dubinin–Radushkevich (DR) equation [4]

$$W = W_{ao} \exp[-(A/\beta E_o)^n] \quad (2)$$

where β is the affinity coefficient and $A = RT\ \ln(p_s/p)$. Following Dubinin's pioneering work [8], different empirical expressions have been suggested, for example by Stoeckli [4]

$$L_o\,(\text{nm}) = 10.8/(E_o - 11.4\,\text{kJ mol}^{-1}). \quad (3)$$

Eq. (3) provides a good estimate for $0.5 < L_o < 1.5$–1.8 nm, but inconsistencies appeared later, due to different factors. One of them is the restricted accessibility of wide pores due to gate effects (entrances being blocked by constrictions or larger pores placed behind smaller pores). This leads to apparent contradictions between the predictions based on E_o and W_o provided by small molecules, and the experimental enthalpies of immersion into bulky liquids. Gate effects may also prevent caffeine from reaching certain pores normally accessible to it. This leads to smaller areas and larger values of L_o. Consequently, we re-examined Eq. (3) by adding computer modelling of CO_2 adsorption [6] and by considering the selective adsorption of phenol [7], which can probe the same micropores as

*Corresponding author. Fax: +41-32-718-2511.
E-mail address: fritz.stoeckli@ich.unine.ch (F. Stoeckli).

0008-6223/01/$ – see front matter © 2001 Elsevier Science Ltd. All rights reserved.
PII: S0008-6223(01)00054-9